

Intraband relaxation of Frenkel excitons in sexithiophene crystals

Piotr Petelenz* and Waldemar Kulig

K. Gumiński Department of Theoretical Chemistry, Jagiellonian University, Ingardena 3, 30-060 Cracow, Poland
(Received 11 May 2009; revised manuscript received 27 August 2009; published 29 September 2009)

A simple theoretical model is used to estimate the rates for relaxation of an exciton optically created in sexithiophene at the top of the exciton band to the emitting state at band bottom. The process is subdivided into three stages; the first two are predicted to be completed within 40 fs while the third (rate-determining) stage takes 500 fs or more. The dependence of the relaxation time on excitation energy is also investigated. The results are in good agreement with available experimental data and suggest further experiments.

DOI: [10.1103/PhysRevB.80.115127](https://doi.org/10.1103/PhysRevB.80.115127)

PACS number(s): 78.40.Me, 71.35.-y, 78.47.jc

I. INTRODUCTION

The imminent applications of organic molecular crystals in optoelectronics create a demand for profound insight into the decay dynamics of excited electronic states optically created in these systems. The dynamic characteristics of electronic excitations are expected to define the branching between Frenkel excitons and the charge-transfer (CT) manifold, critically affecting optical charge-carrier generation,¹ and to set the temporal scale of emission response, potentially important in some applications of light-emitting diodes.²⁻⁴

Experimental investigation of excited-state dynamics in organic molecular crystals is now becoming feasible owing to novel techniques of femtosecond spectroscopy. There is a natural tendency to use these sophisticated methods to study the cases of special interest for potential applications, such as perylene derivatives^{5,6} and oligothiophenes.⁷⁻¹⁰ These latter systems are viewed as especially promising in the technological context, since the lowest excited state (1B_u) of their molecules, polarized parallel to the long molecular axis, is very intense in linear-absorption spectroscopy, guaranteeing a strong coupling between the electronic part of a putative device and the optical radiation field.

The additional bonus is that, apart from their actual applications,¹¹⁻¹⁴ oligothiophenes (nT) are also well suited for model studies.¹⁵⁻¹⁷ In contrast to the situation in perylene derivatives,¹⁸⁻²² their Frenkel (intramolecular) excitons are rather well discernible from their CT states, greatly facilitating the interpretation. Following this line of thought, it is tempting to rationalize the properties of oligothiophene crystal excitations in terms of intramolecular processes alone. This approach was adopted in the pioneering paper of Frolov *et al.*,⁸ where the first measurements of sexithiophene (6T) femtosecond dynamics were reported.

However, this original interpretation was based on an underestimated value of the Davydov splitting in the sexithiophene crystal. In fact, the tentative interpretation⁸ located the upper Davydov component of the lowest sexithiophene excited state at 2.6 eV, instead of 3.45 eV, which is the value accepted nowadays.²³ In that situation the energy span of less than 0.25 eV covered by the exciton band seemed to be marginal on the scale of the processes under consideration (where over an electron volt has to be dissipated), so that crystal-specific channels of excited-state re-

laxation were seemingly of secondary importance. As further studies of other authors revised the initial estimate of the Davydov splitting,²³ the mechanisms of excited-state dynamics in the 6T crystal have to be reconsidered.

The unit cell of the sexithiophene crystal (low-temperature phase) contains four molecules, arranged in two closely spaced pairs, each belonging to a different plane of tight herringbone packing.²⁴⁻³¹ Accordingly, the lowest intramolecular excited state splits into four Davydov components, of which two are symmetry forbidden. Owing to the weakness of the interaction between the tight-packing planes, the two forbidden components are located very close to their allowed counterparts. In effect, the spectra are successfully described in terms of a simplified crystal structure with only two molecules in the unit cell (actually realized in the high-temperature phase of the crystal²⁴⁻³¹).

Due to a peculiar lattice geometry, absorption intensity is concentrated in the upper of the two remaining Davydov components, while the lower component (at about 2.26 eV) is very weak, and consequently its dispersion is marginal. In contrast, the dispersion relation of the upper component (*c* polarized, *D2*), degenerate with the former (*b* polarized, *D1*) at the boundary of the Brillouin zone, spreads all the way to the absorption maximum at about 3.45 eV. Owing to intensity spilling into the continuum of phonon-assisted exciton states off the center of the Brillouin zone,^{32,33} the corresponding absorption band is very broad and diffuse, enabling one to excite the crystal practically at any energy within this enormous interval.

Fluorescence occurs either from the bottom of the *D2* exciton band (with the involvement of an extra phonon to maintain quasimomentum balance) or, more probably, from the lower Davydov component (*D1*). Therefore, if the crystal is excited to a higher energy, the excess energy has to be dissipated in radiationless intraband relaxation. Just the manifestations of this process were experimentally investigated by Frolov *et al.*⁸ and are addressed in the present paper, which provides a theoretical framework needed for interpretation of the pertinent experimental data. Our specific aim is to estimate the efficiency of crystal-specific channels of radiationless relaxation of the intense state observed in the sexithiophene crystal²³ with direct reference to the femtosecond emission and pump-probe measurements of Frolov *et al.*⁷ We hope that the proposed approach may in the future be generalized and applied for other cases.

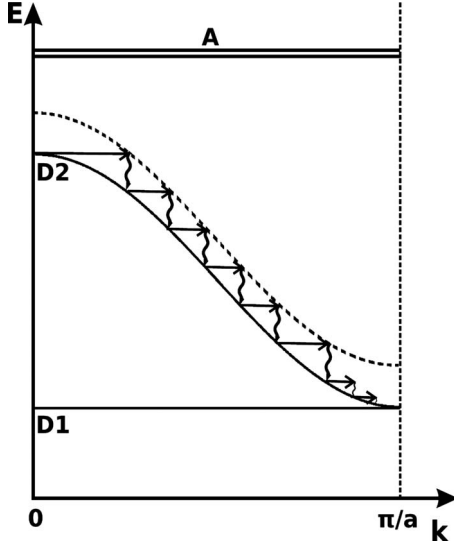


FIG. 1. Schematic band structure of Frenkel excitons in 6T single crystals. *D1* and *D2* represent the two Davydov components of the S_1 state with the broken line showing the one-phonon continuum of *D2*. *A* denotes the two quasidegenerate Davydov components of the Frenkel exciton deriving from the molecular A_g state, with the transition allowed from S_1 , but forbidden from S_0 . Wavy arrows represent phonon energy dissipation.

II. OPTICALLY GENERATED LEVEL AND EXCITON-PHONON CONTINUUM

In the 6T crystal, the dispersion relation of the upper (*c* polarized, *D2*) Davydov component is peaked at the center of the Brillouin zone (as in H aggregates). Therefore, the corresponding discrete crystal level optically generated at quasimomentum $\mathbf{k}=0$ is located at the top of the exciton band and is immersed in the continuum of phonon-accompanied exciton states corresponding to other values of the exciton wave vector (cf. Fig. 1). Those of the unbound exciton-phonon pairs where the phonon quasimomentum exactly cancels the exciton quasimomentum are coupled by weak vibronic interaction to the optically generated $\mathbf{k}=0$ state, making it prone to decay into the continuum.

The decay process is analogous to intramolecular radiationless conversion and has recently been described in similar terms^{32,33} using the analytically solvable Fano model.³⁴ Based on Fano's conclusions, the continua corresponding to different phonon modes were treated jointly, yielding the net lifetime of the discrete state on the order of 3–4 fs.³² In this step, analogous to autoionization, the exciton sheds the energy of one vibrational quantum (which is subsequently dissipated as heat), to end up at the point of its dispersion relation that results from the energy balance. The branching ratio between the decay into exciton-phonon pairs involving different vibrational modes is given by

$$R_i = \frac{S_i \omega_i}{\sum_i S_i \omega_i}, \quad (1)$$

where S_i and ω_i denote the Huang-Rhys parameter and the frequency, respectively, of the i th mode. The relevant param-

TABLE I. Vibrational frequencies (ω_i [cm^{-1}]) and Huang-Rhys (S_i) parameters for sexithiophene (Ref. 35).

i	ω_i	S_i	i	ω_i	S_i
1	105.46	0.35	8	1077.96	0.04
2	143.78	0.09	9	1218.33	0.01
3	291.84	0.01	10	1227.77	0.02
4	307.75	0.20	11	1235.21	0.01
5	703.44	0.17	12	1472.17	0.52
6	726.74	0.01	13	1488.27	0.02
7	1073.14	0.05	14	1547.01	0.03

eters of the dominant 6T modes, resulting from quantum chemistry calculations,³⁵ are listed in Table I, while the diagram of Fig. 2 (top part) depicts the three leading decay pathways; the contributions from other vibrations are smaller by at least an order of magnitude.

III. INTRABAND RELAXATION

The bottom of the exciton band, where from emission may take place, has to be reached by gradual transfer of the exciton energy surplus to phonon modes in consecutive scattering events; this process is referred to as intraband relaxation. It is analogous to the thermalization of charge carriers

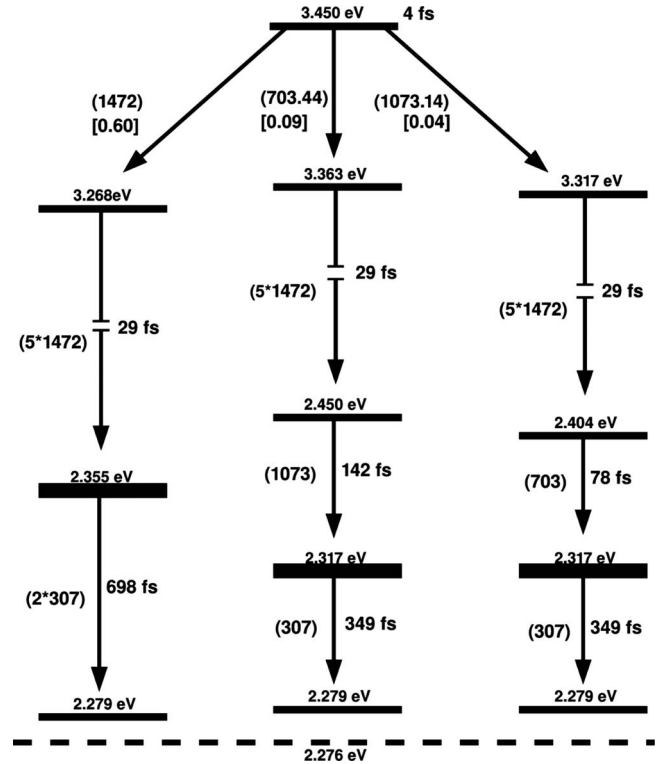


FIG. 2. Relaxation channels of the *D2* state optically created at $\mathbf{k}=0$. Square brackets denote the branching ratio for the decay into the corresponding one-phonon continua. The channels with negligible initial branching fraction and the very slow ones, which reach the band bottom in more than 1000 fs, are not shown.

after their optical generation, already treated in the past within a scheme appropriate for weak vibronic coupling,¹ which is directly adopted here. As derived there, with the density of states assumed approximately constant throughout the exciton band, the Fermi golden rule yields a simple expression for the thermally averaged rate W of exciton scattering from the state with energy E to the state with energy $E - \hbar\omega_i$, accompanied by the release of the phonon $\hbar\omega_i$. This expression reads¹

$$W = 2\pi \frac{S_i \hbar \omega_i^2}{\Delta}, \quad (2)$$

where Δ is the width of the exciton band. [Note that, consistently with Eq. (1) but in contrast to the notation of Ref. 1, S_i is expressed in dimensionless units.]

Equation (2) describes the rate of exciton energy loss per vibrational quantum, which (upon multiplication by $\hbar\omega_i$) may be readily converted to energy units. This demonstrates that the molecular vibrations that substantially contribute to the depletion of exciton energy must be characterized by a substantial shift of the normal coordinate upon electronic excitation and by a large frequency. Accordingly, Table I allows one to identify several vibrational modes as the potentially leading energy sinks.

The excess energy E of the exciton with respect to the bottom of the band may be depleted by generating (alternatively) various phonon sequences. The channel involving exclusively the 1472 cm^{-1} mode is by far the most effective; direct calculation proves the rate constants for other modes to be lower by at least an order of magnitude. This pathway of relaxation starts independently from each of the three off-center excitons originally generated by the decay of the $\mathbf{k}=0$ discrete state and continues until the exciton energy with respect to the band bottom is less than one vibrational quantum of the dominant 1472 cm^{-1} mode. Then lower-frequency modes are taking over; the specific sequence of scattering events that turns out to be the most effective in further relaxation depends on the precise energy at the bottom of each dissipation ladder of the 1472 cm^{-1} mode. In Fig. 2 we show only the leading depletion pathways because other channels are again slower at least by an order of magnitude. All the channels naturally terminate when the remaining energy surplus is smaller than the vibrational quantum of the lowest-frequency mode.

Figure 2 summarizes the dominant relaxation pathways obtained within the model described above for optical excitation tuned strictly to the experimental energy of the upper Davydov component. The diagram shows the energies of the states involved, the number of dissipated vibrational quanta of the specified frequency (in parenthesis) and the requisite times, calculated as reciprocals of the corresponding rates. The branching fractions for the decay of the initial $\mathbf{k}=0$ state are shown in square brackets.

IV. INTERPRETATION OF STIMULATED-EMISSION EXPERIMENTS

According to the diagram, the three distinctive steps of relaxation are characterized by different time constants: the

decay of the discrete state into one of the alternative phonon continua takes about 4 fs, to be followed by rapid dissipation of the energy of the thereby created off-center exciton into five quanta of the 1472 cm^{-1} vibration (30 fs); finally the remaining energy is slowly dissipated into low-frequency, weakly coupled modes (400–700 fs). Essentially the same scenario is found for optical excitation in the diffuse onset of the main absorption peak, i.e., at energies lower, but still exceeding one quantum of the strongly coupled high-frequency mode: the difference is merely in the time interval needed for the second step, which is then proportionally shorter, depending on the number of quanta to be released.

The third step, i.e., depletion of the residual exciton energy into the lower-frequency weakly coupled modes, is the slowest one and determines the overall relaxation rate. Its duration is predetermined by the energy of the vibrational quantum released in the first step, which sets the precise amount of energy to be dissipated in the last step: the process is faster if the energy interval closely fits a small number of quanta of reasonably effective accepting mode(s), the effectiveness in this regard being a compromise between the mode's frequency (preferably large) and its coupling constant.

Overall, the dominant relaxation channel starts from the discrete state at 3.45 eV with the release of one quantum of the 1472 cm^{-1} mode into the corresponding continuum, which takes about 4 fs. In about 30 fs, subsequent scattering accompanied by creation of five more phonons of the same kind leads to the state at 2.355 eV, which further decays by releasing two quanta of the 307 cm^{-1} vibration. The 2.355 eV state is the actual bottleneck; the fastest pathway of its depletion has the characteristic time on the order of 700 fs, so that the total time from the outset to produce the completely relaxed state is about 730 fs.

Although the alternative decay of the discrete 3.45 eV state into the one-phonon continuum of the 703 cm^{-1} mode is considerably less probable in view of the smaller coupling constant (resulting in a small branching fraction), this (initially slower) relaxation pathway is temporally competitive in a long run, since the residual energy (0.174 eV) left after the release of 5 quanta of the 1472 cm^{-1} vibration is easier to convert into the modes of lower frequencies (1073 cm^{-1} and subsequently 308 cm^{-1}). In effect, this channel is faster, leading to the bottom of the $D2$ band in less than 530 fs from the moment when the discrete state was optically generated.

Globally, the fastest is the third alternative pathway, still slightly less probable at the first stage. The initial decay produces one quantum of the 1073 cm^{-1} mode, again followed by the release of 5 quanta of the 1472 cm^{-1} vibration. Finally, the resultant 2.404 eV state is deactivated, releasing in a sequence one 703 cm^{-1} quantum and one 308 cm^{-1} quantum, which yields 460 fs as the total relaxation time from the initial discrete state.

In reality, the emitting state is the other (b polarized, $D1$) Davydov component. However, its dispersion is practically negligible (as depicted in Fig. 2) owing to the small transition dipole moment, while the surfaces representing the two components touch at the border of the Brillouin zone. In effect, final relaxation to the emitting $D1$ state takes approximately the same time as that needed to reach the bottom of

the $D2$ band (at the border of the Brillouin zone) since the mechanism is similar and the same amount of energy has to be dissipated. Accordingly, the above simplistic estimate should be roughly correct. These results are in excellent agreement with the experimental fact that stimulated emission starts about 0.5 ps after excitation,⁸ which perfectly fits our estimate of the relaxation time for the fastest channel (460 fs), and is close to that for the dominant channel (730 fs).

V. INTERPRETATION OF PUMP-PROBE EXPERIMENTS

An alternative method of investigating excited-state dynamics is femtosecond pump-probe spectroscopy. The 6T molecule has an A_g state at about 3.6 eV,³⁶ accessible by a dipole-allowed transition from S_1 ; its energy perfectly matches the experimentally observed absorption of probe photons at 1.25–1.3 eV, assuming that the crystalline samples pumped at 2.5–3 eV have relaxed (almost) to the bottom of the S_1 exciton band.⁸ In contrast to stimulated emission, photoinduced absorption (PA) starts practically instantaneously, i.e., within the experimental resolution of 150 fs after excitation. According to the original interpretation,⁸ complete exciton thermalization is needed for emission but is not necessary for PA.

Our present results show this finding in a new light. As the transition to the A_g state from the ground state is dipole forbidden, the exciton resonance interaction (mediated predominantly by the dipole-dipole term) is marginal, giving rise to a flat dispersion relation, parallel to that of the lower ($D1$) Davydov component of the S_1 state. In effect, the vertical excitation energy from $D1$ to the A_g state is equal at any point of the Brillouin zone and also the same as that needed for analogous excitation from the bottom of the $D2$ exciton band (i.e., at the border of the Brillouin zone, cf. Fig. 1). The long-lived states, represented in Fig. 2 by the thick lines, are located only slightly (less than 0.2 eV) above the band bottom. Their energies perfectly fit the onset observed in the spectral dependence of the PA signal.⁸

This spectral dependence was recorded 5 ps after excitation. We attribute the main PA peak observed there at 1.25–1.3 eV to the transition from the completely relaxed $D1/D2$ exciton populated via all the pathways discussed above. In contrast, we tentatively associate the practically instantaneous photoinduced absorption with the low-energy PA onset, starting about 0.2 eV below the main peak; the latter value is consistent with the residual energies (with respect to the band bottom) of the incompletely relaxed, rapidly populated $D2$ states (thick lines in Fig. 2).

VI. RELAXATION PROCESS VIEWED BY ALTERNATIVE TECHNIQUES

Accordingly, the following scenario may be envisaged for the relaxation of the optically generated upper Davydov component at 3.45 eV. The decay of the discrete state into the continuum occurs in 4 fs, releasing one phonon, with the probability of populating the individual modes given by the branching ratio R_i defined above. This opens several inde-

pendent channels of relaxation, each starting at the energy set by the frequency of the mode in hand. Further decay is rapid as long as high-frequency modes characterized by large Franck-Condon parameters are engaged; this stage takes about 30 fs (i.e., well within the temporal resolution of 150 fs of the pump-probe experiments⁸). The thereby generated states, located less than 0.2 eV above the bottom of the exciton band, live considerably longer, giving rise to the low-energy onset of the main peak of the photoinduced absorption signal; however, their lifetimes are still much too short to enable them to contribute significantly to the observed emission.

When the residual energy is less than one quantum of the most depletion-effective mode, the relaxation process slows down. The fastest route leading to the emitting state at the band bottom has the characteristic time of 460 fs, in fair agreement with the observed delay of the stimulated emission signal (0.5 ps); it is our conjecture that the main 1.25 eV peak in the PA spectrum should also appear just after this time, in contrast to the PA onset at the energy lower by about 0.2 eV, presumably appearing after about 30 fs, as mentioned above.

VII. DEPENDENCE ON EXCITATION ENERGY—CALCULATIONS

We have already mentioned two aspects of the dependence of the relaxation process on the energy of the initial state generated by optical absorption. On the one hand, the dissipation of the surplus exciton energy by scattering on phonons is obviously the faster the smaller is the number of phonons to be generated. As the 1472 cm^{-1} is the leading energy sink, the relaxation time decreases stepwise at the energies corresponding to the multiples of this frequency. The decrease is relatively mild, on the order of 6 fs per quantum.

On the other hand, the net intraband decay rate critically depends on the residual energy to be deposited in less dissipation-effective modes. As just the depletion of this residue is ultimately the bottleneck of the process as a whole, a relatively small difference in the energy of the initial state may result in a dramatic change in the total relaxation time. For some energy values where the final relaxation step is mediated by the modes characterized by small displacements upon electronic excitation, the total decay time may well reach thousands of femtoseconds. In contrast, when the energy to be dissipated amounts exactly to a multiple of the dominant 1472 cm^{-1} vibration, the process may be readily completed within a few tens of femtoseconds. This is illustrated in Fig. 3 showing the dependence (calculated at 0.005 eV resolution) of the total relaxation time on the energy of the initial optically generated state. Understandably, the histograms slightly differ for the most probable channel and for the fastest channel but the qualitative picture is very much the same. Experimentally, the dependence is probably somewhat smoother owing to the finite spectral width of the vibronic levels involved.

VIII. DEPENDENCE ON EXCITATION ENERGY—EXPERIMENTAL EVIDENCE

The gist of the above expectations is corroborated by the experimental data of Refs. 9 and 10, where additional infor-

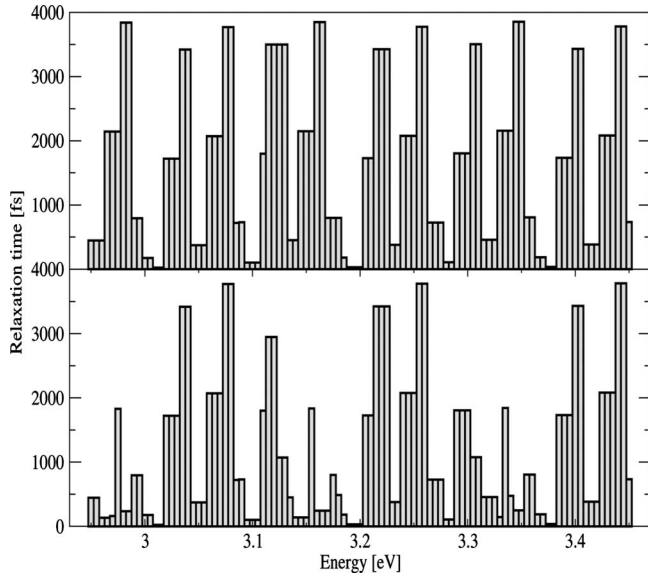


FIG. 3. Dependence of the total intraband-relaxation time on the energy of the initial optically generated state. Top panel: most probable channel; bottom panel: fastest channel.

mation on relaxation times was reported. Loi *et al.*⁹ used a frequency-doubled 1.53 eV laser (so that the sexithiophene crystal was excited at 3.06 eV), and observed fluorescence to appear after $120(\pm 20)$ fs, while in the measurements of Cordella *et al.*¹⁰ the second harmonic of a 1.61 eV laser was used (with the net exciting light energy of 3.22 eV), and fluorescence was reported to occur after 300–400 fs. This latter relaxation time is quite close to that reported by Frolov *et al.*⁸ (about 500 fs) but the former one at the first glance might seem drastically discordant.

Actually, in view of the results presented in Fig. 3, taken at conceptual level, this dramatic discrepancy was only to be expected. Admittedly, at quantitative level the relaxation times predicted for the precise excitation energies used in the experiments evidently deviate from those reported.^{9,10} This is not surprising for several reasons. In the first place, the experiments mentioned above probe the frequencies on the energy surface of the excited electronic state while the frequencies reported in Ref. 35 pertain to the ground state; second, the calculated frequencies are subject to the inherent errors of the applied quantum chemistry methods. Moreover, the actual energies of individual vibronic levels are also affected by vibronic interactions, since the scheme of weak vibronic coupling used throughout this paper (where the ensuing shifts are neglected), nearly exact for the upper Davydov component, is admittedly less accurate^{37,38} for lower vibronic levels.

The importance of these factors is probably considerably exaggerated in Ref. 9 where the relaxation times are interpreted in terms of an effective mode with frequency of 1258 cm^{-1} . Nevertheless, it does seem reasonable to suppose that the calculated frequency of 1472 cm^{-1} is in reality lower. If a correction of the order of $50\text{--}60\text{ cm}^{-1}$ per vibrational quantum is assumed, the 102 fs relaxation time predicted by the calculation for the excitation energy of 3.10 eV shifts down to 3.06 eV, in perfect agreement with the experi-

mental value (120 fs for this energy). It is equally tempting to associate the relaxation time of 300–400 fs, observed at 3.22 eV, with the neighboring slot of the histogram (3.23 eV); in that case, the agreement is again perfect.

Taking the above conjectures with a grain of salt, one has to realize that the interpretational difficulties are compounded by an additional complication, stemming from the fact that in the experiments reported in Refs. 9 and 10 the crystal is excited at energies (3–3.25 eV) where the absorption spectrum is virtually structureless,³⁹ containing contributions from different states, the most important being the one-phonon continua of different vibrational modes^{32,33} and the bound exciton-phonon states (vibrons) deriving from various phonon combinations.^{37,40} All of them are subject to further radiationless relaxation and may be the actual precursors of the observed fluorescence.

The precise vibrational parentage of the actually generated state is crucial for further temporal evolution, as it defines the relaxation channels and the pertinent coupling constants. Suppose that the exciting light is tuned to the energy of a state characterized by a very long relaxation time (e.g., at 3.07–3.08 eV, cf. Fig. 3), resulting from the small Huang-Rhys parameter of one or more of the excited vibrational modes it entails. These same parameters also govern (via the Franck-Condon factor) the intensity of the corresponding optical transition, which is then negligible.

However, owing to the finite width of all the states under consideration (consistently neglected in this paper), at the same energy the exciting light will very likely hit also the tail of an absorption band due to a nearby more intense state, ultimately populating a level characterized by a larger Franck-Condon factor, which implies larger Huang-Rhys parameters of the relevant modes and a shorter relaxation time. In this way, direct optical excitation (in contrast to the radiationless decay of the upper Davydov component described in Sec. II) seems to favor creation of the states characterized by relatively shorter lifetimes.

IX. DISCUSSION

The present interpretation is an alternative to that proposed by the authors of Ref. 2 on the spur of their original experimental results, where the observed effects were rationalized in terms of intramolecular vibrational relaxation. At that time, there was a tendency to underestimate the Davydov splitting in 6T, locating the upper component at 2.6 eV, instead of 3.45 eV (which is the value accepted nowadays²³). Accordingly, the erstwhile explanation based on intramolecular vibrational relaxation needs to be reconsidered in the new context.

The model used to obtain the present results is admittedly simplistic. It is rooted in the approximation of weak vibronic coupling, partially justified for the upper Davydov component at $\mathbf{k}=0$ by the results of numerical calculations performed for finite clusters³⁸ and for an infinite crystal,^{40,41} demonstrating that the upper Davydov component created in 6T is practically a free exciton, accompanied by only marginal lattice deformation. This is also true for the high-energy vibronic replicas of the lower Davydov component

(with several quanta of the main progression-forming mode).⁴¹ Admittedly, toward the bottom of the *D2* band and in the *D1* vibronic manifold this approximation is expected to be gradually losing validity.^{38,40} Our estimates in this region are less reliable also on account of the simplified representation of the vibrational density of states, equivalent to a sum of delta functions. The natural blurring of their contours would make the dependence of the rates on the energies of the bottleneck states smoother. In order to improve the description of the final relaxation stages it would also be necessary to include more phonon modes including the intermolecular ones. Nevertheless, major deviations from the predicted overall behavior and time scale are rather unlikely since the amount of energy left to be dissipated is quite small. This expectation is confirmed by tentative calculations.

The scenario offered in this paper agrees with the available experimental data and is open to further verification. The estimated time scale of the initial stages of intraband relaxation (30 fs) is on the order of the times measured for analogous processes in perylene-3,4,9,10-tetracarboxylic-3,4,9,10-dianhydride and N,N'-di-

methylperylene-3,4:9,10-bis(dicarboimide),⁵ i.e., within the reach of state-of-the-art experiments. The assignment of the instantaneous PA signal to the nontotally-relaxed states about 0.2 eV above the band bottom could be tested by a pump-probe experiment with higher spectral resolution. The expected result is that with the probe beam tuned to about 1.05–1.1 eV (to match the energy interval between the pertinent states and the A_g state), the PA signal should appear within 30–40 fs, while for the probe beam tuned exactly to the bottom of the band, the signal should appear roughly at the same time as stimulated emission (500–1000 fs). We hope that our present estimates will inspire this kind of experimental studies. Almost equally tantalizing seems to be a systematic study of the dependence of the intraband-relaxation time on excitation energy.

ACKNOWLEDGMENTS

The authors express their enormous gratitude to the reviewer for bringing Refs. **9** and **10** to their attention. Were it not for this inspiration, Secs. **VII** and **VIII** of this paper would not have been conceived.

*petelenz@chemia.uj.edu.pl

- ¹P. Petelenz and D. Mucha, *J. Chem. Phys.* **100**, 4607 (1994).
- ²M. Mazzeo, V. Vitale, F. D. Sala, D. Pisignano, M. Anni, G. Barbarella, L. Favaretto, A. Zanelli, R. Cingolani, and G. Gigli, *Adv. Mater. (Weinheim, Ger.)* **15**, 2060 (2003).
- ³F. Demanze, J. Cornil, F. Garnier, G. Horowitz, P. Valat, A. Yassar, R. Lazzaroni, and J.-L. Brdas, *J. Phys. Chem.* **101**, 4553 (1997).
- ⁴M. Mazzeo, D. Pisignano, L. Favaretto, G. Sotgiub, G. Barbarella, R. Cingolani, and G. Gigli, *Synth. Met.* **139**, 675 (2003).
- ⁵E. Engel, M. Koschorreck, K. Leo, and M. Hoffmann, *J. Lumin.* **112**, 299 (2005).
- ⁶E. Engel, Ph.D. thesis, Technische Universität Dresden, 2005.
- ⁷S. V. Frolov, C. Kloc, S. Berg, G. A. Thomas, and B. Batlogg, *Chem. Phys. Lett.* **326**, 558 (2000).
- ⁸S. V. Frolov, C. Kloc, B. Batlogg, M. Wohlgenannt, X. Jiang, and Z. V. Vardeny, *Phys. Rev. B* **63**, 205203 (2001).
- ⁹M. A. Loi, A. Mura, G. Bongiovanni, Q. Cai, C. Martin, H. R. Chandrasekhar, M. Chandrasekhar, W. Graupner, and F. Garnier, *Phys. Rev. Lett.* **86**, 732 (2001).
- ¹⁰F. Cordella, R. Orru, M. A. Loi, A. Mura, and G. Bongiovanni, *Phys. Rev. B* **68**, 113203 (2003).
- ¹¹*Handbook of Conducting Polymers*, edited by T. A. Scotheim (Marcel Dekker, New York, 2007), Vols. 1 and 2.
- ¹²*Handbook of Oligo- and Poly-Thiophenes*, edited by D. Fichou (Wiley-VCH, Weinheim, 1999).
- ¹³G. Horowitz, D. Fichou, X. Peng, Z. Xu, and F. Garnier, *Solid State Commun.* **72**, 381 (1989).
- ¹⁴A. Dodabalapur, L. Torsi, and H. E. Katz, *Science* **268**, 270 (1995).
- ¹⁵Z. Zhao and F. C. Spano, *J. Chem. Phys.* **122**, 114701 (2005).
- ¹⁶F. C. Spano, *J. Chem. Phys.* **116**, 5877 (2002).
- ¹⁷Z. Zhao and F. C. Spano, *J. Phys. Chem. C* **111**, 6113 (2007).
- ¹⁸M. H. Hennessy, Z. G. Soos, R. A. Pascal, Jr., and A. Girlando, *Chem. Phys.* **245**, 199 (1999).
- ¹⁹M. Hoffmann and Z. G. Soos, *Phys. Rev. B* **66**, 024305 (2002).
- ²⁰M. Andrzejak, G. Mazur, and P. Petelenz, *J. Mol. Struct.* **527**, 91 (2000).
- ²¹G. Mazur and P. Petelenz, *Chem. Phys. Lett.* **324**, 161 (2000).
- ²²G. Mazur, P. Petelenz, and M. Slawik, *J. Chem. Phys.* **118**, 1423 (2003).
- ²³M. A. Loi, C. Martin, H. R. Chandrasekhar, M. Chandrasekhar, W. Graupner, F. Garnier, A. Mura, and G. Bongiovanni, *Phys. Rev. B* **66**, 113102 (2002).
- ²⁴D. Fichou, *J. Mater. Chem.* **10**, 571 (2000).
- ²⁵M. Pelletier and F. Brisse, *Acta Crystallogr., Sect. C: Cryst. Struct. Commun.* **50**, 1942 (1994).
- ²⁶F. van Bolhuis, H. Wynberg, E. E. Havinga, E. W. Meijer, and E. G. J. Starring, *Synth. Met.* **30**, 381 (1989).
- ²⁷T. Siegrist, C. Kloc, R. A. Laudise, H. E. Katz, and R. C. Haddon, *Adv. Mater. (Weinheim, Ger.)* **10**, 379 (1998).
- ²⁸L. Antolini, G. Horowitz, F. Kouki, and F. Garnier, *Adv. Mater. (Weinheim, Ger.)* **10**, 382 (1998).
- ²⁹G. Horowitz, B. Bachet, A. Yassar, P. Lang, F. Demanze, J. L. Fave, and F. Garnier, *Chem. Mater.* **7**, 1337 (1995).
- ³⁰T. Siegrist, R. M. Fleming, R. C. Haddon, R. A. Laudise, A. J. Lovinger, H. E. Katz, P. Bridenbaugh, and D. D. Davis, *J. Mater. Res.* **10**, 2170 (1995).
- ³¹D. Fichou, B. Bachet, F. Demanze, I. Billy, G. Horowitz, and F. Garnier, *Adv. Mater. (Weinheim, Ger.)* **8**, 500 (1996).
- ³²P. Petelenz and W. Kulig, *Chem. Phys.* **343**, 100 (2008).
- ³³W. Kulig and P. Petelenz, *Phys. Rev. B* **79**, 094305 (2009).
- ³⁴U. Fano, *Phys. Rev.* **124**, 1866 (1961).
- ³⁵M. Andrzejak and M. Pawlikowski, *J. Phys. Chem. A* **112**, 13737 (2008).

- ³⁶R. Colditz, D. Gerbner, M. Helbig, and S. Rentsch, *Chem. Phys.* **201**, 309 (1995).
- ³⁷F. C. Spano, L. Silvestri, P. Spearman, L. Raimondo, and S. Tavazzi, *J. Chem. Phys.* **127**, 184703 (2007).
- ³⁸F. C. Spano, *J. Chem. Phys.* **118**, 981 (2003).
- ³⁹S. Tavazzi, M. Laicini, L. Raimondo, P. Spearman, A. Borghesi, A. Papagni, and S. Trabattoni, *Appl. Surf. Sci.* **253**, 296 (2006).
- ⁴⁰A. Stradomska and P. Petelenz, *J. Chem. Phys.* **130**, 094705 (2009).
- ⁴¹A. Stradomska and P. Petelenz, *J. Chem. Phys.* **131**, 044507 (2009).